IEICE TRANS. COMMUN., VOL.E91–B, NO.6 JUNE 2008

PAPER

Iterative Overlap FDE for Multicode DS-CDMA

Kazuaki TAKEDA[†a)], ***Member***, **Hiromichi TOMEBA**[†], ***Student Member***, ***and*** **Fumiyuki ADACHI**[†], ***Fellow***

SUMMARY Recently, a new frequency-domain equalization (FDE) technique, called overlap FDE, that requires no GI insertion was proposed. However, the residual inter/intra-block interference (IBI) cannot completely be removed. In addition to this, for multicode direct sequence code division multiple access (DS-CDMA), the presence of residual inter-chip interference (ICI) after FDE distorts orthogonality among the spreading codes. In this paper, we propose an iterative overlap FDE for multicode DS-CDMA to suppress both the residual IBI and the residual ICI. In the iterative overlap FDE, joint minimum mean square error (MMSE)-FDE and ICI cancellation is repeated a sufficient number of times. The bit error rate (BER) performance with the iterative overlap FDE is evaluated by computer simulation.

key words: *DS-CDMA, MMSE frequency-domain equalization, ICI cancellation, overlap FDE*

1. Introduction

With the growing mobile wireless communication market, there has been a tremendous demand for high-speed data services [1]. The wireless channel is composed of many distinct propagation paths having different time delays, resulting in a frequency-selective fading channel [2]. Direct sequence code division multiple access (DS-CDMA) using rake combining is used in the present cellular mobile communication systems for data transmissions of up to around a few Mbps [3], [4]. Recently, a lot of research attention is paid to the next generation mobile communication systems that will support data services of higher than several tens of Mbps. The wireless channel for high speed data transmission is severely frequency-selective and the bit error rate (BER) performance with the rake combining degrades due to a strong inter-path interference. Hence, an advanced equalization technique is indispensable.

Recently, it was shown [5]–[8] that frequency-domain equalization (FDE) based on the minimum mean square error (MMSE) criterion can provide much better BER performance of DS-CDMA than the rake combining in a severe frequency-selective channel. In DS-CDMA with MMSE-FDE, the insertion of the guard interval (GI) is necessary to avoid inter-block interference from the previous block and intra-block interference of its own block. However, the transmission efficiency is reduced by the GI insertion. A cyclic prefix (CP) reconstruction technique was proposed to suppress both the inter-block interference and intra-block interference in [9]. Recently, overlap FDE has been proposed in [10], [11] to suppress the residual inter/intra-block interference (IBI) after MMSE-FDE. Since, in overlap FDE, the inter-block interference and intra-block interference need not separately be treated unlike [9], the terminology 'IBI' is used in this paper to represent the inter/intra-block interference. The impulse response of MMSE-FDE filter does not spread over the entire FFT block. Hence, the residual IBI after MMSE-FDE is present only at the edge of the FFT block. This fact can be exploited to avoid the GI insertion. By overlapping consecutive FFT blocks and picking up a middle $M(\leq N_c)$-chip part of N_c-chip block after MMSE-FDE, the residual IBI can be suppressed (this technique is called overlap FDE). However, overlap FDE cannot completely remove the residual IBI. In addition, the presence of the residual inter-chip interference (ICI) after FDE distorts orthogonality among the spreading codes. The residual IBI and the residual ICI degrade the downlink BER performance as the code multiplexing order increases.

The frequency-domain interference cancellation for DS-CDMA uplink was proposed in [12]. Recently, we proposed a joint MMSE-FDE and frequency-domain ICI cancellation to improve the BER performance of the DS-CDMA downlink transmission [13]. However, in [12], [13], DS-CDMA with the GI insertion is considered.

In this paper, we propose an iterative overlap FDE for multicode DS-CDMA to suppress both the residual IBI and the residual ICI. In the iterative overlap FDE, after joint MMSE-FDE and ICI cancellation is repeated a sufficient number of times to suppress the residual ICI, a middle M-chip part of N_c-chip block is picked up to suppress the residual IBI. If the residual ICI is sufficiently suppressed by the ICI cancellation, the MMSE weight approaches the maximum ratio combining (MRC) weight. The impulse response of MRC-FDE filter is concentrated in close vicinity to the edge of an FFT block. Hence, the residual IBI can be sufficiently suppressed by the iterative overlap FDE.

Remainder of this paper is organized as follows. Section 2 presents the conventional overlap FDE and shows that the performance degradation from the theoretical lower bound is mainly due to the residual IBI and the residual ICI. In Sect. 3, to suppress both the residual IBI and the residual ICI, the iterative overlap FDE is proposed. In Sect. 4, the achievable BER performance of the iterative overlap FDE in a frequency-selective Rayleigh fading channel is evaluated by computer simulation. Section 5 offers some conclusions.

Manuscript received July 5, 2007.
Manuscript revised December 25, 2007.

[†]The authors are with the Dept. of Electrical and Communication Engineering, Graduate School of Engineering, Tohoku University, Sendai-shi, 980-8579 Japan.
a) E-mail: takeda@mobile.ecei.tohoku.ac.jp

DOI: 10.1093/ietcom/e91–b.6.1942

Copyright © 2008 The Institute of Electronics, Information and Communication Engineers

2. Conventional Overlap FDE

In this section, we investigate the impulse response of MMSE-FDE filter to explain why overlap FDE can work successfully without requiring the GI insertion. After the transmission system model using overlap FDE is presented, the simulated BER performance using overlap FDE is shown.

2.1 Impulse Response of MMSE-FDE Filter

The simulation parameters are summarized in Table 1. We assume QPSK data modulation, an FFT block size of N_c=256 chips. The channel is assumed to be a frequency-selective block Rayleigh fading channel having a chip-spaced L=16-path uniform power delay profile. Perfect chip timing and ideal channel estimation are assumed.

One shot observation of the impulse response of MMSE-FDE filter is shown in Fig. 1. The impulse response does not spread over the entire FFT block of N_c chips. Therefore, the residual IBI after MMSE-FDE is present only close to the edge of the FFT block if the maximum time delay of the multipath channel is much shorter than the FFT block size. This is exploited by overlap FDE. The consecutive FFT blocks are overlapped as shown in Fig. 2, and a middle $M(\leq N_c)$-chip part of N_c-chip block is picked up after MMSE-FDE. In this way, MMSE-FDE can be carried out without inserting the GI.

Table 1 Simulation parameters.

Transmitter	Modulation	QPSK
	Number of FFT points	N_c=256
	Spreading sequence	Product of Walsh sequence and PN sequence
	Spreading factor	SF=1,16
Channel	Fading	Frequency -selective block Rayleigh fading
	Power delay profile	L=16-path uniform power delay profile
Receiver	Frequency-domain equalization	MMSE
	Channel estimation	Ideal

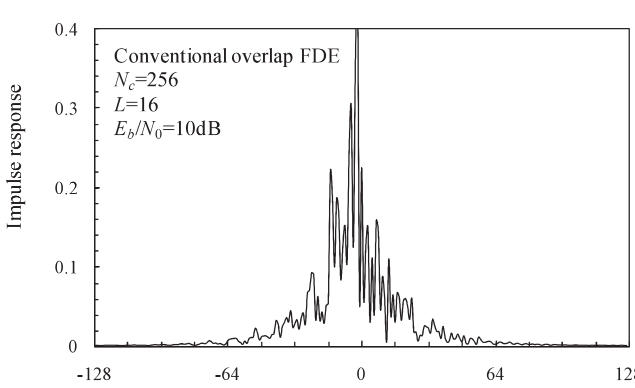

Fig. 1 One shot obsevation of the impulse response of MMSE-FDE filter.

2.2 Transmission System Model

The transmission system model for multicode DS-CDMA with conventional overlap FDE is illustrated in Fig. 3. At the transmitter, a binary data sequence is firstly data modulated and then, serial/parallel (S/P) converted to U parallel data sequences. The uth data modulated symbol sequence is then spread by multiplying it with an orthogonal spreading sequence. The resultant U chip sequences are multiplexed and further multiplied by a common scramble sequence to make the resultant multicode DS-CDMA signal like white-noise.

The multicode DS-CDMA signal is transmitted over a frequency-selective fading channel and is received at a receiver. The received chip sequence is decomposed by N_c-point FFT into N_c frequency components. Note that the consecutive FFT blocks are overlapped as shown in Fig. 2. After MMSE-FDE is carried out, inverse FFT (IFFT) is applied to obtain the time-domain received chip sequence. A middle M-chip part of N_c-chip block is picked up. Finally, a sequence of M-chip block is despread to recover the received data.

2.3 Simulated BER Performance

The simulated BER performance of multicode DS-CDMA with overlap FDE is plotted for various values of M in Fig. 4 as a function of the average received bit energy-to-additive white Gaussian noise (AWGN) power spectrum density ratio E_b/N_0, defined as $E_b/N_0 = 0.5SF(E_c/N_0)$, where SF is the spreading factor and E_c/N_0 is the average chip energy-to-AWGN power spectrum density ratio. The spreading factor SF is assumed to be SF=16 and the code multiplexing order U is the same as SF. For comparison, the theoretical lower bound [8] and the BER performance of DS-CDMA with a GI of $N_g = 32$ are also plotted (the GI insertion loss in E_b/N_0 is taken into account). The BER performance of overlap FDE is close to that with the GI in a lower E_b/N_0 region, but a BER floor still exists due to the residual IBI. A big performance gap is seen between the theoretical lower bound and the BER performance with overlap FDE. Even with the GI (i.e., no IBI is present), the performance gap is as much as 7.7 dB for BER = 10^{-4}. The reason for this is given as follows. Zero-forcing (ZF)-FDE aims to perform the perfect restoration of frequency-nonselective channel, but produces the noise enhancement. However, MMSE-

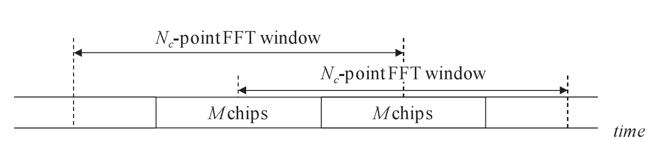

Fig. 2 Received signal sequence and FFT window.

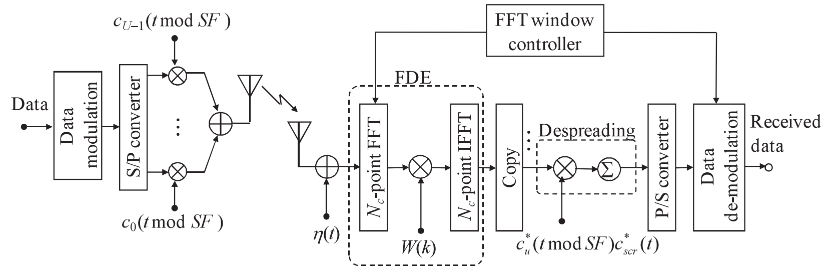

(a) Transmitter (b) Receiver

Fig. 3 Transmission system model of conventional overlap FDE.

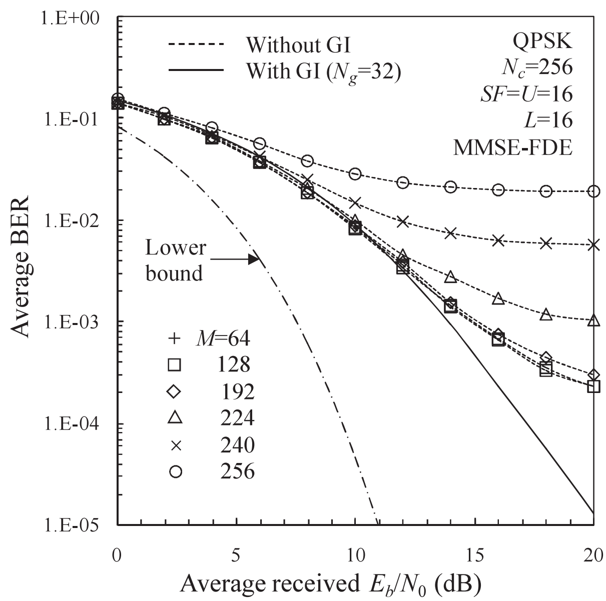

Fig. 4 BER performance with overlap FDE ($SF = U = 16$).

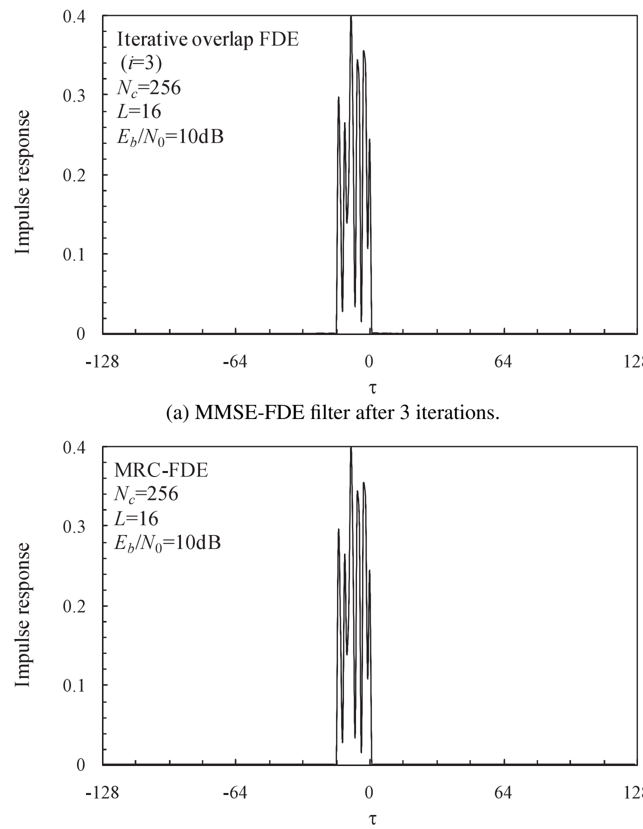

(a) MMSE-FDE filter after 3 iterations.

(b) MRC-FDE filter.

Fig. 5 One shot obsevation of the impulse response of MMSE-FDE filter after 3 iterations and MRC-FDE filter.

FDE mitigates the noise enhancement by giving up the perfect restoration of the frequency-non-selective channel. The performance degradation from the theoretical lower-bound is due to the presence of the residual ICI and slightly increased noise power (because the noise enhancement cannot be completely mitigated).

3. Proposed Iterative Overlap FDE

In this paper, we propose the iterative overlap FDE to sufficiently suppress both the residual IBI and the residual ICI. In the iterative overlap FDE, after joint MMSE-FDE and ICI cancellation is repeated a sufficient number of times to suppress the residual ICI, a middle M-chip part of N_c-chip block is picked up to suppress the residual IBI. As the number of iterations increases, the FDE weight approaches the maximum ratio combining (MRC) weight since the residual ICI can be better suppressed [13]. Figure 5(a) shows one shot observation of the impulse response of MMSE-FDE filter after 3 iterations, which is seen to be much closer to the impulse response of MRC-FDE filter (this can be understood by comparing Figs. 5(a) and (b)). The impulse response concentrates in close vicinity to $\tau = 0$ compared to that of the original MMSE-FDE filter (compare Fig. 1 and Fig. 5(a)). This suggests that the residual IBI can be much reduced by the iterative overlap FDE compared to the conventional overlap FDE, thereby reducing the error floor caused by the residual IBI.

3.1 Transmission System Model

The transmission system model for multicode DS-CDMA with the iterative overlap FDE is illustrated in Fig. 6. At the transmitter, a binary data sequence is firstly data modulated and then, S/P converted to U parallel data sequences. The uth data modulated symbol sequence $d_u(n)$, $u = 0 \sim U-1$, is then spread by multiplying it with an orthogonal spreading sequence $c_u(t)$. The resultant U chip sequences are multiplexed and further multiplied by a common scramble sequence $c_{scr}(t)$. Finally, the $SF \times M$ row-column chip interleaving is applied.

At the receiver, the received chip sequence is decomposed by N_c-point FFT into N_c frequency components. Note that the consecutive FFT blocks are overlapped as shown in Fig. 2. MMSE-FDE is carried out, and then, ICI cancellation is performed in the frequency-domain. IFFT is applied to obtain the time-domain received chip sequence. After chip deinterleaving is applied, despreading, log-likelihood ratio (LLR) computation and soft symbol replica generation are carried out. The soft symbol replica is respread and chip-interleaved for updating the residual ICI replica. Re-spreading of erroneous symbol replica results in error propagation over consecutive SF chips. To avoid this, chip interleaving is used after spreading. Joint MMSE-FDE and ICI cancellation is repeated a sufficient number of times. A middle M-chip part of N_c-chip block is picked up. Finally, a sequence of M-chip block is despread to recover the received data.

3.2 Transmit and Receive Signals

Throughout this paper, chip-spaced time representation of the transmitted signals is used. At the transmitter, the spread chip sequence is interleaved by the SF-by-M block chip-interleaver. The spread and interleaved signal chip sequence $\{\hat{s}(t);\ t = \ldots, -1, 0, 1, \ldots\}$ to be transmitted can be expressed, using the equivalent lowpass representation, as

$$\hat{s}(t) = \sqrt{\frac{2E_c}{T_c}}\, s(t), \tag{1}$$

where E_c and T_c denote the chip energy and the chip duration, respectively, and $s(t)$ is given by

$$s(t) = \left[\sum_{u=0}^{U-1} d_u\left(\lfloor t/SF \rfloor\right) c_u(t \bmod SF)\right] c_{scr}(t) \tag{2}$$

with $|c_u(t)| = |c_{scr}(t)| = 1$, where $\lfloor x \rfloor$ represents the largest integer smaller than or equal to x.

The propagation channel is assumed to be an L-path frequency-selective block fading channel. The impulse response $h(\tau)$ of a multipath channel can be expressed as [14]

$$h(\tau) = \sum_{l=0}^{L-1} h_l \delta(\tau - \tau_l), \tag{3}$$

where h_l and τ_l are the complex-valued path gain and time delay of the lth path ($l = 0 \sim L-1$), respectively, with $\sum_{l=0}^{L-1} E[|h_l|^2] = 1$ ($E[.]$ denotes the ensemble average operation). The received chip sequence $\{r(t);\ t = \ldots, -1, 0, 1, \ldots\}$ can be expressed as

$$r(t) = \sqrt{\frac{2E_c}{T_c}} \sum_{l=0}^{L-1} h_l s(t - \tau_l) + \eta(t), \tag{4}$$

where $\eta(t)$ is a zero-mean complex Gaussian process with a variance of $2N_0/T_c$ with N_0 being the single-sided power spectrum density of the AWGN process.

Without loss of generality, we assume the detection of an $SF \times M$-interleaved chip sequence. The N_c-point FFT block is applied to the received chip sequence $r(t)$ so that M chips of interest is placed at the center of the FFT block. For simplicity, we have assumed that the path gains remain constant over at least SF FFT blocks. The mth ($m = 0 \sim SF-1$) FFT block can be expressed, using $r(t)$, as $\{r_m(t) = r(t + mM - (N_c - M)/2);\ t = 0 \sim N_c - 1\}$ (see Fig. 8). For performing FDE, the desired signal component must be expressed as a circular convolution between the channel impulse response and the transmitted N_c-chip block over $t = 0 \sim N_c - 1$. Since the GI is not inserted, the IBI component appears. $r_m(t)$, $m = 0 \sim SF - 1$, can be expressed as

$$r_m(t) = \sqrt{\frac{2E_c}{T_c}} \sum_{l=0}^{L-1} h_l s_m((t-\tau_l) \bmod N_c) + \nu_m(t) + \eta_m(t), \tag{5}$$

where $s_m(t) = s(t + mM - (N_c - M)/2)$, $t = 0 \sim N_c - 1$, and $\nu_m(t)$ is the IBI component and is given by

$$\nu_m(t) = \sqrt{\frac{2E_c}{T_c}} \sum_{l=0}^{L-1} h_l \{s_{m-1}(t + M - \tau_l) - s_m((t - \tau_l) \bmod N_c)\} \times \{u_0(t) - u_0(t - \tau_l)\} \tag{6}$$

with

$$u_0(t) = \begin{cases} 1, & t \geq 0 \\ 0, & t < 0 \end{cases}. \tag{7}$$

In Eq. (6), $s_{m-1}(t + M - \tau_l)\{u_0(t) - u_0(t - \tau_l)\}$ is the inter-block interference from the $(m-1)$th block and $s_m((t - \tau_l) \bmod N_c)\{u_0(t) - u_0(t - \tau_l)\}$ is the intra-block interference of the mth block itself as shown in Fig. 7. In this paper, the terminology 'IBI' is used to represent the inter/intra-block interference as stated in Sect. 1.

3.3 Joint MMSE-FDE and ICI Cancellation

Joint MMSE-FDE and ICI cancellation is repeated in an iterative fashion. Below, the ith iteration is described.

N_c-point FFT is applied to decompose $\{r_m(t);\ t = 0 \sim N_c - 1\}$ into N_c frequency components $\{R_m(k);\ k = 0 \sim N_c - 1\}$. The kth frequency component $R_m(k)$ can be written as

$$\begin{aligned} R_m(k) &= \sum_{t=0}^{N_c-1} r_m(t) \exp\left(-j2\pi k \frac{t}{N_c}\right) \\ &= \sqrt{\frac{2E_c}{T_c}} H(k) S_m(k) + N_m(k) + \Pi_m(k), \end{aligned} \tag{8}$$

where $S_m(k)$, $H(k)$, $N_m(k)$ and $\Pi_m(k)$ are the kth frequency component of $\{s_m(t);\ t = 0 \sim N_c - 1\}$, the channel gain, the IBI component and the noise component, respectively. They are given by

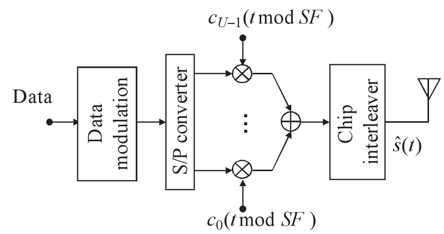

(a) Transmitter.

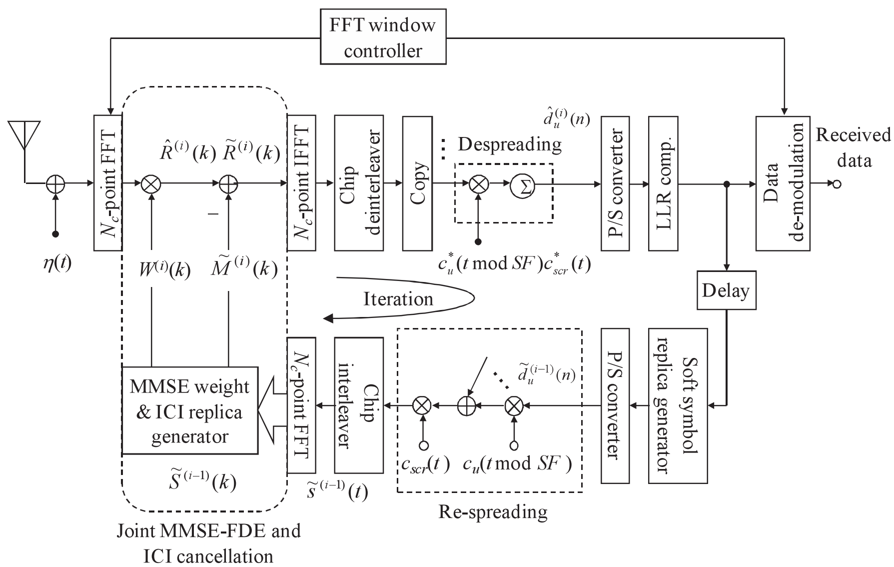

(b) Receiver with iterative overlap FDE.

Fig. 6 Transmitter/receiver strucutre.

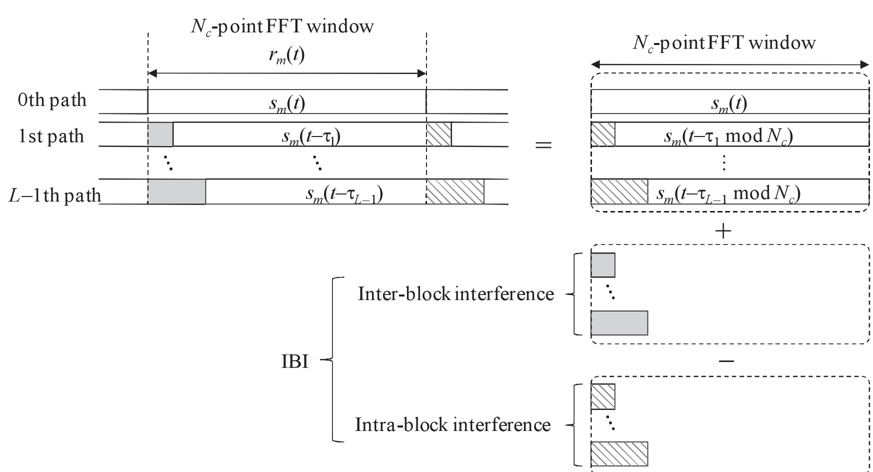

Fig. 7 IBI component.

$$\begin{cases} S_m(k) = \sum_{t=0}^{N_c-1} s_m(t)\exp\left(-j2\pi k\frac{t}{N_c}\right) \\ H(k) = \sum_{l=0}^{L-1} h_l \exp\left(-j2\pi k\frac{\tau_l}{N_c}\right) \\ N_m(k) = \sum_{t=0}^{L-1} \nu_m(t)\exp\left(-j2\pi k\frac{t}{N_c}\right) \\ \Pi_m(k) = \sum_{t=0}^{N_c-1} \eta_m(t)\exp\left(-j2\pi k\frac{t}{N_c}\right) \end{cases}. \quad (9)$$

MMSE-FDE is carried out as follows:

$$\hat{R}_m^{(i)}(k) = R_m(k)W_m^{(i)}(k) = \sqrt{\frac{2E_c}{T_c}}S_m(k)\hat{H}_m^{(i)}(k) + \hat{N}_m^{(i)}(k) + \hat{\Pi}_m^{(i)}(k) \quad (10)$$

with

$$\begin{cases} \hat{H}_m^{(i)}(k) = W_m^{(i)}(k)H(k) \\ \hat{N}_m^{(i)}(k) = W_m^{(i)}(k)N_m(k) \\ \hat{\Pi}_m^{(i)}(k) = W_m^{(i)}(k)\Pi_m(k) \end{cases}, \quad (11)$$

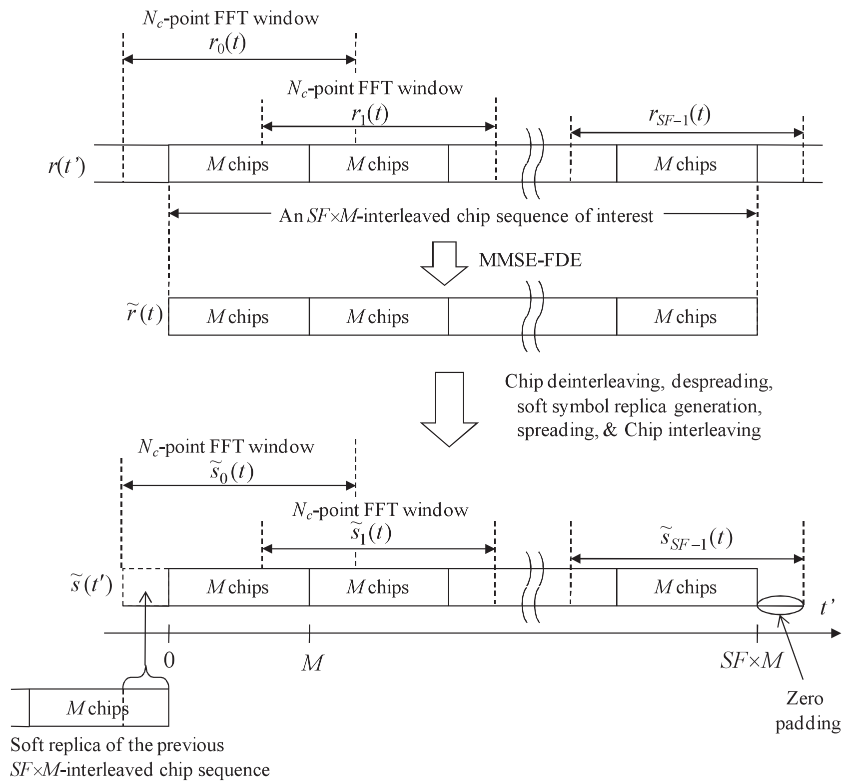

Fig. 8 Iterative overlap FDE and soft replica generation.

where $W_m^{(i)}(k)$ is the MMSE weight for the ith iteration and $\hat{H}_m^{(i)}(k)$, $\hat{N}_m^{(i)}(k)$ and $\hat{\Pi}_m^{(i)}(k)$ are the equivalent channel gain, the residual IBI and the noise after MMSE-FDE, respectively. $W_m^{(i)}(k)$ is given as [13]

$$W_m^{(i)}(k) = \frac{H^*(k)}{\rho_m^{(i-1)}\,|H(k)|^2 + \left(\frac{E_c}{N_0}\right)^{-1} + \tilde{\sigma}_{IBI}^2}, \tag{12}$$

where $\rho_m^{(i-1)}$ is an interference factor [13] and $\rho_m^{(-1)} = 1$. The computation of $\rho_m^{(i-1)}$ for $i > 0$ is explained in Sect. 3.5. $\tilde{\sigma}_{IBI}^2$ is the IBI power normalized by E_c/T_c.

ICI cancellation is performed as

$$\tilde{R}_m^{(i)}(k) = \hat{R}_m^{(i)}(k) - \tilde{M}_m^{(i)}(k), \tag{13}$$

where $\tilde{M}_m^{(i)}(k)$ is the residual ICI replica, and is given by [13]

$$\tilde{M}_m^{(i)}(k) = \begin{cases} 0 & \text{for } i = 0 \\ \sqrt{\frac{2E_c}{T_c}}\left\{\hat{H}_m^{(i)}(k) - A_m^{(i)}\right\}\tilde{S}_m^{(i-1)}(k) & \text{for } i \geq 1 \end{cases}, \tag{14}$$

where $\tilde{S}_m^{(i-1)}(k)$ is the kth frequency component of the replica of the transmitted chip sequence, which is generated by feeding back a decision variable of the $(i-1)$th iteration stage and $A_m^{(i)}$ is given by

$$A_m^{(i)} = \frac{1}{N_c}\sum_{k'=0}^{N_c-1}\hat{H}_m^{(i)}(k'). \tag{15}$$

3.4 Despreading

N_c-point IFFT is applied to transform the frequency-domain signal $\{\tilde{R}_m^{(i)}(k);\ k = 0 \sim N_c - 1\}$ into the time-domain chip sequence $\{\tilde{r}_m^{(i)}(t);\ t = 0 \sim N_c - 1\}$:

$$\begin{aligned}\tilde{r}_m^{(i)}(t) &= \frac{1}{N_c}\sum_{k=0}^{N_c-1}\tilde{R}_m^{(i)}(k)\exp\left(j2\pi t\frac{k}{N_c}\right) \\ &= \sqrt{\frac{2E_c}{T_c}}A_m^{(i)}s_m(t) + \mu_m^{(i)}(t) + \hat{\nu}_m^{(i)}(t) + \hat{\eta}_m^{(i)}(t),\end{aligned} \tag{16}$$

where $s_m(t)$ in the first term represents the transmitted chip sequence, $\mu_m^{(i)}(t)$ is the residual ICI, $\hat{\nu}_m^{(i)}(t)$ is the residual IBI and $\hat{\eta}_m^{(i)}(t)$ is the noise.

An M-chip central part of each N_c-chip block is picked up. This is repeated for SF blocks to obtain an $SF \times M$-chip sequence $\{\tilde{r}^{(i)}(t);\ t = 0 \sim SF \times M - 1\}$ (see Fig. 8). $\tilde{r}^{(i)}(t)$ is expressed, using $\tilde{r}_m^{(i)}(t)$, as

$$\tilde{r}^{(i)}(t + mM) = \tilde{r}_m^{(i)}\,(t + (N_c - M)/2) \tag{17}$$

for $m = 0 \sim SF - 1$ and $t = 0 \sim M - 1$.

After chip deinterleaving, despreading is carried out on $\tilde{r}^{(i)}(t)$, $t = 0 \sim SF \times M - 1$, to obtain

$$\hat{d}_u^{(i)}(n) = \frac{1}{SF}\sum_{t=nSF}^{(n+1)SF-1}\tilde{r}^{(i)}(t)c_u^*(t \bmod SF)c_{scr}^*(t) \tag{18}$$

for $n = 0 \sim M - 1$.

3.5 MMSE-FDE Weight Updateing and the Residual ICI Replica Generation

The soft decision variable is used to generate the replica $\{\tilde{s}_m^{(i-1)}(t);\ t=0\sim N_c-1\}$ of the transmitted chip sequence. Using $\hat{d}_u^{(i-1)}(n)$, the log-likelihood ratio (LLR) for the xth bit in the nth symbol $d_u(n)$ $(n=0\sim M-1)$, where $x=0\sim \log_2 K-1$ and K is the modulation level, can be computed as [15]

$$L_u^{(i-1)}(n,x) = \ln\left(\frac{p_u^{(i-1)}(b_{n,x}=1)}{p_u^{(i-1)}(b_{n,x}=0)}\right) \approx \frac{\left|\hat{d}_u^{(i-1)}(n)-\sqrt{2E_c/T_c}A^{(i-1)}d^{\min}_{b_{n,x}=0}\right|^2}{2\left(\hat{\sigma}^{(i-1)}\right)^2} - \frac{\left|\hat{d}_u^{(i-1)}(n)-\sqrt{2E_c/T_c}A^{(i-1)}d^{\min}_{b_{n,x}=1}\right|^2}{2\left(\hat{\sigma}^{(i-1)}\right)^2}, \quad (19)$$

where $p_u^{(i-1)}$ $(b_{n,x}=0$ (or 1)) is a posteriori probability of $b_{n,x}=0$ (or 1) and $d^{\min}_{b_{n,x}=0}$ (or $d^{\min}_{b_{n,x}=1}$) is the most probable symbol that gives the minimum Euclidean distance from $\hat{d}_u^{(i-1)}(n)$ among all candidate symbols $\{d\}$ with $b_{n,x}=0$ (or 1). $A^{(i-1)}=(1/SF)\sum_{m=0}^{SF-1}A_m^{(i-1)}$ is the average of $A_m^{(i-1)}$ over $m=0\sim SF-1$. In Eq. (19), $2\left(\hat{\sigma}^{(i-1)}\right)^2$ is the variance of the noise plus residual ICI. $2\left(\hat{\sigma}^{(i-1)}\right)^2$ is given by

$$2\left(\hat{\sigma}^{(i-1)}\right)^2 = \frac{1}{SF}\sum_{m=0}^{SF-1}2\left(\hat{\sigma}_m^{(i-1)}\right)^2, \quad (20)$$

where $2\left(\hat{\sigma}_m^{(i-1)}\right)^2$ is given by [13].

$$2\left(\hat{\sigma}_m^{(i-1)}\right)^2 = \frac{1}{SF}\left[\frac{2N_0}{T_c}\frac{1}{N_c}\sum_{k=0}^{N_c-1}|W_m^{(i-1)}(k)|^2 + \frac{2E_c}{T_c}\rho_m^{(i-2)}\left\{\frac{1}{N_c}\sum_{k=0}^{N_c-1}|\hat{H}_m^{(i-1)}(k)|^2-\left|A_m^{(i-1)}\right|^2\right\}\right]. \quad (21)$$

The soft symbol replica $\tilde{d}_u^{(i-1)}(n)$, $n=0\sim M-1$, can be obtained from [16]

$$\tilde{d}_u^{(i-1)}(n) = \sum_{d\in D} d\prod_{b_{n,x}\in d}p_u^{(i-1)}(b_{n,x}), \quad (22)$$

where D denotes a set of $\{d\}$ and $p_u^{(i-1)}(b_{n,x}=0)$ and $p_u^{(i-1)}(b_{n,x}=1)$ are given, from Eq. (19), as

$$\begin{cases} p_u^{(i-1)}(b_{n,x}=0) = -\frac{1}{2}\tanh\left(\frac{L_u^{(i-1)}(n,x)}{2}\right)+\frac{1}{2} \\ p_u^{(i-1)}(b_{n,x}=1) = \frac{1}{2}\tanh\left(\frac{L_u^{(i-1)}(n,x)}{2}\right)+\frac{1}{2} \end{cases} \quad (23)$$

since $p_u^{(i-1)}(b_{n,x}=1)+p_u^{(i-1)}(b_{n,x}=0)=1$.

For QPSK data modulation, Eq. (22) becomes

$$\tilde{d}_u^{(i-1)}(n) = \frac{1}{\sqrt{2}}\tanh\left(\frac{L_u^{(i-1)}(n,0)}{2}\right) + j\frac{1}{\sqrt{2}}\tanh\left(\frac{L_u^{(i-1)}(n,1)}{2}\right). \quad (24)$$

Using $\{\tilde{d}_u^{(i-1)}(n);\ n=0\sim M-1\}$, $\rho_m^{(i-1)}$ in Eq. (12) can be computed as

$$\rho_m^{(i-1)} = \frac{1}{M}\sum_{n=0}^{M-1}\sum_{u=0}^{U-1}\left\{E\left[|d_u(n)|^2\right]-\left|\tilde{d}_u^{(i-1)}(n)\right|^2\right\} \text{ for all } m, \quad (25)$$

where $E[|d_u(n)|^2]$ is the expectation value of $d_u(n)$ for the given $\hat{d}_u^{(i-1)}(n)$. $E[|d_u(n)|^2]$ is computed, using Eq. (23), as

$$E[|d_u(n)|^2] = \sum_{d\in D}|d|^2\prod_{b_{n,x}\in d}p_u^{(i-1)}(b_{n,x}) = 1 \text{ for QPSK.} \quad (26)$$

The replica $\{\tilde{s}^{(i-1)}(t);\ t=0\sim SF\times M-1\}$ of the transmitted chip sequence $s(t)$ is generated as

$$\tilde{s}^{(i-1)}(t) = \left[\sum_{u=0}^{U-1}\tilde{d}_u^{(i-1)}(\lfloor t/SF\rfloor)\ c_u(t \bmod SF)\right]c_{scr}(t). \quad (27)$$

After chip interleaving, the N_c-point FFT block is applied to $\tilde{s}^{(i-1)}(t)$. The mth chip block replica $\{\tilde{s}_m^{(i-1)}(t),\ m=0\sim SF-1,\ t=0\sim N_c-1\}$ can be expressed, using $\tilde{s}^{(i-1)}(t)$, as (see Fig. 8)

$$\tilde{s}_m^{(i-1)}(t) = \tilde{s}^{(i-1)}\left(t+mM-(N_c-M)/2\right). \quad (28)$$

Owing to overlap FDE, the chip block replica $\tilde{s}_m^{(i-1)}(t)$ is almost free from the residual IBI for $m=1\sim SF-2$. However, as can be understood from Fig. 8, $\tilde{s}_0^{(i-1)}(t)$ and $\tilde{s}_{SF-1}^{(i-1)}(t)$ suffer from the residual IBI since the residual IBI comes from the previous and next $SF\times M$-interleaved chip sequences, respectively. Therefore, $\tilde{s}_0^{(i-1)}(t)$, $t=0\sim(N_c-M)/2-1$, is generated using the decision result of the previous $SF\times M$-interleaved chip sequence, while $\tilde{s}_{SF-1}^{(i-1)}(t)$, $t=(N_c+M)/2\sim N_c-1$, is generated by zero-padding.

N_c-point FFT is applied to decompose the replica $\{\tilde{s}_m^{(i-1)}(t);\ t=0\sim N_c-1\}$ into N_c frequency components $\{\tilde{S}_m^{(i-1)}(k);\ k=0\sim(N_c-1)\}$ as

$$\tilde{S}_m^{(i-1)}(k) = \sum_{t=0}^{N_c-1}\tilde{s}_m^{(i-1)}(t)\exp\left(-j2\pi k\frac{t}{N_c}\right). \quad (29)$$

Substituting Eq. (29) into Eq. (14), we obtain the frequency-domain ICI replica $\tilde{M}_m^{(i)}(k)$.

3.6 Residual IBI after ICI Cancellation

Assume that the residual ICI is perfectly cancelled (i.e., $\tilde{S}_m^{(i-1)}(k)=S_m(k)$ and $\tilde{s}_m^{(i-1)}(t)=s_m(t)$). Since $\rho_m^{(i-1)}=0$ as understood from Eq. (25), the MMSE weight of Eq. (12) approaches the MRC weight given by

$$W_m^{(i)}(k) = H^*(k). \quad (30)$$

Using Eqs. (10)–(14), the frequency-domain signal $\{\tilde{R}_m^{(i)}(k);$

$k = 0 \sim N_c - 1\}$ after MRC-FDE and perfect ICI cancellation is given by

$$\tilde{R}_m^{(i)}(k) = \sqrt{\frac{2E_c}{T_c}} A_m^{(i)} S_m(k) + H^*(k) N_m(k) + H^*(k) \Pi_m(k). \tag{31}$$

The frequency-domain signal $\{\tilde{R}_m^{(i)}(k);\ k = 0 \sim N_c - 1\}$ is transformed into time-domain chip sequence $\{\tilde{r}_m^{(i)}(t);\ t = 0 \sim N_c - 1\}$ by applying N_c-point IFFT:

$$\tilde{r}_m^{(i)}(t) = \sqrt{\frac{2E_c}{T_c}} A_m^{(i)} s(t) + \hat{v}_m(t) + \hat{\eta}_m(t), \tag{32}$$

where $\hat{v}_m(t)$ is the residual IBI given by

$$\begin{aligned}\hat{v}_m(t) &= \frac{1}{N_c} \sum_{k=0}^{N_c-1} H^*(k) N_m(k) \exp\left(j2\pi t \frac{k}{N_c}\right) \\ &= \sum_{l=0}^{L-1} h_l^* v_m(t + \tau_l \bmod N_c).\end{aligned} \tag{33}$$

Since $v_m(t) = 0$ for $t > \tau_{L-1}$, Eq. (33) can be rewritten as

$$\hat{v}_m(t) = \begin{cases} 0 & \tau_{L-1} < t < N_c - \tau_{L-1} \\ \sum_{l=0}^{L-1} h_l^* v_m(t + \tau_l \bmod N_c) & \text{otherwise} \end{cases}. \tag{34}$$

It can be understood from Eq. (34) that, if the residual ICI is perfectly cancelled, the residual IBI is not present in an interval of $\tau_{L-1} < t < N_c - \tau_{L-1}$. Hence, the residual IBI can be avoided by picking up the received chip sequence of an interval of $\tau_{L-1} < t < N_c - \tau_{L-1}$.

4. Computer Simulation

The simulation parameters are the same as in Table 1. The simulated BER performance with the iterative overlap FDE is plotted in Fig. 9 with the number i of iterations as a parameter for $M = 160$. We assume the spreading factor $SF = 1$ and 16 and $U = SF$. For comparison, theoretical lower bound is also plotted. The BER performance of $i = 0$ corresponds to the case of overlap FDE. The iterative overlap FDE can significantly improve the BER performance, while the BER floor due to the residual IBI is seen for overlap FDE ($i = 0$). A good BER performance is achieved for $i = 3$. When $SF = 1$, the required E_b/N_0 reduction is as much as 5.1 dB for BER $= 10^{-3}$. The E_b/N_0 degradation from the theoretical lower bound is only 1.2 dB. When $SF = U = 16$, the BER performance is greatly improved by the iterative overlap FDE, similar to the case of $SF = 1$. The E_b/N_0 degradation is as small as 0.9 dB from the theoretical lower bound.

The BER performance achievable by the iterative overlap FDE may depend on the degree of the channel frequency-selectivity. The BER performance of full-code multiplexed DS-CDMA with the iterative overlap FDE ($i = 3$) is plotted in Fig. 10 with the number L of paths as a parameter. When $i = 0$ (i.e., conventional overlap FDE), better BER performance is seen for larger L in a low E_b/N_0 region since the frequency diversity gain gets larger. However, in a high E_b/N_0 region, as L increases, the BER performance becomes worse due to the larger residual IBI. However, when $i = 3$, a very good BER performance is achieved by the iterative overlap FDE and no BER floor is seen irrespective of L. As L increases, the BER performance improves since the iterative overlap FDE can suppress both the residual IBI and residual ICI while achieving the frequency diversity gain.

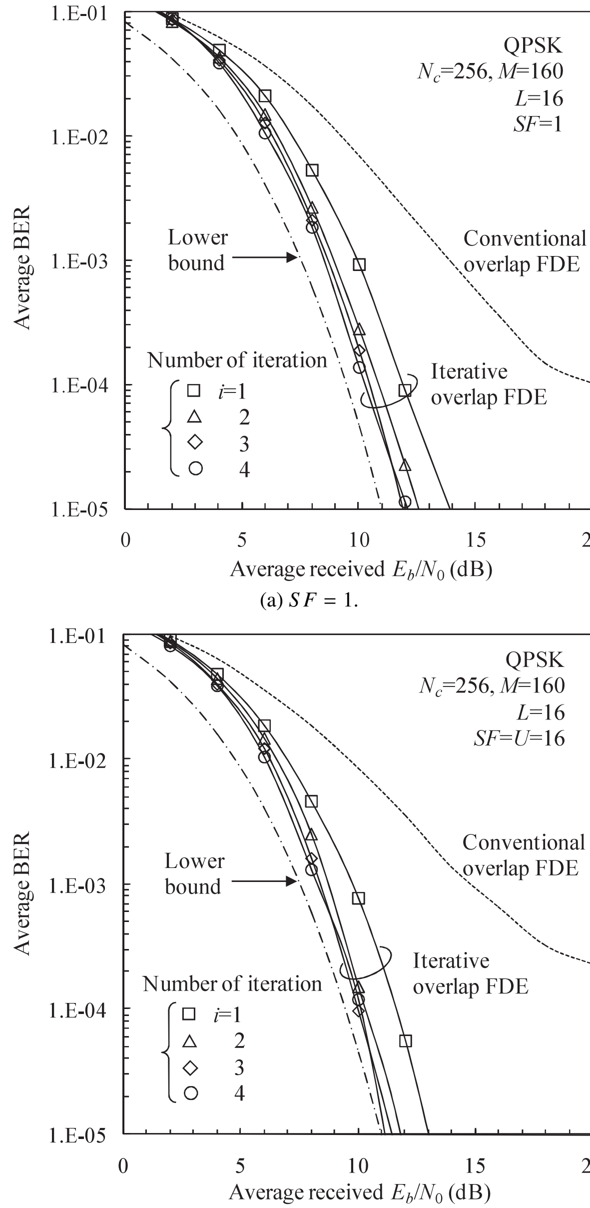

(a) $SF = 1$.

(b) $SF = U = 16$.

Fig. 9 BER performance with iterative overlap FDE.

5. Conclusion

Although overlap FDE can improve the BER performance of DS-CDMA without the GI, the BER floor exists due to the residual IBI. The residual ICI is also present after

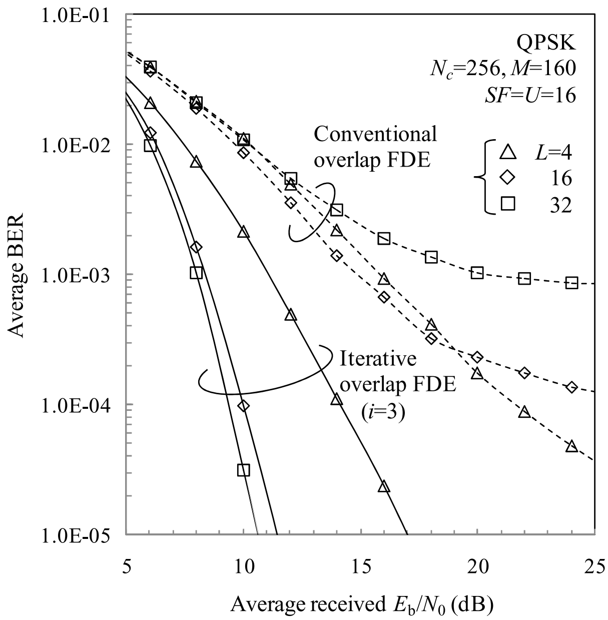

Fig. 10 Effect of the channel frequency-selectivity.

MMSE-FDE, which is the predominant cause of performance degradation from the theoretical lower bound. In this paper, an iterative overlap FDE was proposed. In the iterative overlap FDE, after joint MMSE-FDE and ICI cancellation is repeated a sufficient number of times to suppress the residual ICI, a middle M-chip part of N_c-chip block is picked up to suppress the residual IBI. The BER performance with the iterative overlap FDE was evaluated by computer simulation. The iterative overlap FDE can significantly improve the BER performance irrespective of the degree of the channel frequency-selectivity. It was shown that, when $L = 16$ and $SF = U = 1$ (16), the E_b/N_0 reduction from the performance with $i = 0$ is as much as about 5.1 (6.4) dB for achieving BER = 10^{-3}. The E_b/N_0 degradation from the theoretical lower bound is only 1.2 (0.9) dB for $SF = U = 1$ (16). Performance comparison between the iterative overlap FDE and the CP reconstruction technique is left as an interesting future study.

References

[1] F. Adachi, "Wireless past and future — Evolving mobile communications systems," IEICE Trans. Fundamentals, vol.E83-A, no.1, pp.55–60, Jan. 2001.
[2] W.C. Jakes, Jr., ed., Microwave mobile communications, Wiley, New York, 1974.
[3] F. Adachi, M. Sawahashi, and H. Suda, "Wideband DS-CDMA for next generation mobile communications systems," IEEE Commun. Mag., vol.36, no.9, pp.56–69, Sept. 1998.
[4] J.G. Proakis, Digital communications, 3rd ed., McGraw-Hill, 1995.
[5] F.W. Vook, T.A. Thomas, and K.L. Baum, "Cyclic-prefix CDMA with antenna diversity," Proc. IEEE VTC 2002 Spring, pp.1002–1006, Birmingham, U.S.A., May 2002.
[6] F. Adachi, T. Sao, and T. Itagaki, "Performance of multicode DS-CDMA using frequency domain equalization in a frequency selective fading channel," Electron. Lett., vol.39, no.2, pp.239–241, Jan. 2003.
[7] I. Martoyo, G.M.A. Sessler, J. Luber, and F.K. Jondral, "Comparing equalizers and multiuser detections for DS-CDMA downlink systems," Proc. IEEE VTC 2004-Spring, pp.1649–1653, Milan, Italy, May 2004.
[8] F. Adachi, D. Garg, S. Takaoka, and K. Takeda, "Broadband CDMA techniques," IEEE Wireless Commun. Mag., vol.12, no.2, pp.8–18, April 2005.
[9] Y. Li, S. McLaughlin, and D.G.M. Gruickshank, "Bandwidth efficient single carrier systems with frequency domain equalisation," Electron. Lett., vol.41, no.15, pp.857–858, July 2005.
[10] I. Martoyo, T. Weiss, F. Capar, and F.K. Jondral, "Low complexity CDMA downlink receiver based on frequency domain equalization," Proc. IEEE VTC 2003-Fall, pp.987–991, Florida, U.S.A., Oct. 2003.
[11] K. Takeda, H. Tomeba, and F. Adachi, "DS-CDMA frequency-domain equalization with inter-block interference suppression," IEICE Technical Report, RCS2005-17, May 2005.
[12] S. Tomasin and N. Benvenuto, "Equalization and multiuser interference cancellation in CDMA systems," Proc. 6th International Symposium on Wireless Personal Multimedia Communication (WPMC), vol.1, pp.10–14, Yokosuka, Japan, Oct. 2003.
[13] K. Takeda, K. Ishihara, and F. Adachi, "Downlink DS-CDMA transmission with joint MMSE equalization and ICI cancellation," Proc. IEEE VTC 2006-Spring, pp.1762–1766, Melbourne, Australia, May 2006.
[14] T.S. Rappaport, Wireless communications, Prentice Hall, 1996.
[15] A. Stefanov and T. Duman, "Turbo coded modulation for wireless communications with antenna diversity," Proc. IEEE VTC99-Fall, pp.1565–1569, Netherlands, Sept. 1999.
[16] X. Wang and H.V. Poor, "Iterative (turbo) soft interference cancellation and decoding for coded CDMA," IEEE Commun. Mag., vol.47, no.7, pp.1046–1060, July 1999.

Kazuaki Takeda received his B.E., M.S. and Dr.Eng. degrees in communications engineering from Tohoku University, Sendai, Japan, in 2003, 2004 and 2007 respectively. Currently he is a postdoctoral fellow at the Department of Electrical and Communications Engineering, Graduate School of Engineering, Tohoku University. Since 2005, he has been a Japan Society for the Promotion of Science (JSPS) research fellow. His research interests include equalization, interference cancellation, transmit/receive diversity, and multiple access techniques. He was a recipient of the 2003 IEICE RCS (Radio Communication Systems) Active Research Award and 2004 Inose Scientific Encouragement Prize.

Hiromichi Tomeba received his B.S. and M.S. degree in communications engineering from Tohoku University, Sendai, Japan, in 2004 and 2006. Currently he is a Japan Society for the Promotion of Science (JSPS) research fellow, studying toward his Ph.D. degree at the Department of Electrical and Communications Engineering, Graduate School of Engineering, Tohoku University. His research interests include frequency-domain equalization and antenna diversity techniques for mobile communication systems. He was a recipient of the 2004 and 2005 IEICE RCS (Radio Communication Systems) Active Research Award.

Fumiyuki Adachi received the B.S. and Dr.Eng. degrees in electrical engineering from Tohoku University, Sendai, Japan, in 1973 and 1984, respectively. In April 1973, he joined the Electrical Communications Laboratories of Nippon Telegraph & Telephone Corporation (now NTT) and conducted various types of research related to digital cellular mobile communications. From July 1992 to December 1999, he was with NTT Mobile Communications Network, Inc. (now NTT DoCoMo, Inc.), where he led a research group on wideband/broadband CDMA wireless access for IMT-2000 and beyond. Since January 2000, he has been with Tohoku University, Sendai, Japan, where he is a Professor of Electrical and Communication Engineering at the Graduate School of Engineering. His research interests are in CDMA wireless access techniques, equalization, transmit/receive antenna diversity, MIMO, adaptive transmission, and channel coding, with particular application to broadband wireless communications systems. From October 1984 to September 1985, he was a United Kingdom SERC Visiting Research Fellow in the Department of Electrical Engineering and Electronics at Liverpool University. Dr. Adachi served as a Guest Editor of IEEE JSAC on Broadband Wireless Techniques, October 1999, Wideband CDMA I, August 2000, Wideband CDMA II, Jan. 2001, and Next Generation CDMA Technologies, Jan. 2006. He is an IEEE Fellow and was a co-recipient of the IEEE Vehicular Technology Transactions Best Paper of the Year Award 1980 and again 1990 and also a recipient of Avant Garde award 2000. He is an IEICE Fellow and was a recipient of IEICE Achievement Award 2002 and a co-recipient of the IEICE Transactions Best Paper of the Year Award 1996 and again 1998. He was a recipient of Thomson Scientific Research Front Award 2004.